

Published in final edited form as:

Nature. ; 478(7367): 114–118. doi:10.1038/nature10490.

Endonuclease G is a novel determinant of cardiac hypertrophy and mitochondrial function

Chris McDermott-Roe¹, Junmei Ye², Rizwan Ahmed¹, Xi-Ming Sun¹, Anna Serafin³, James Ware¹, Leonardo Bottolo¹, Phil Muckett¹, Xavier Cañas³, Jisheng Zhang², Glenn C. Rowe⁴, Rachel Buchan¹, Han Lu¹, Adam Braithwaite¹, Massimiliano Mancini⁵, David Hauton⁶, Ramon Martí⁷, Elena García-Arumí⁷, Norbert Hubner^{8,9}, Howard Jacob¹⁰, Tadao Serikawa¹¹, Vaclav Zidek¹², Frantisek Papousek¹², Frantisek Kolar¹², Maria Cardona², Marisol Ruiz-Meana¹³, David García-Dorado¹³, Joan X Comella¹⁴, Leanne E Felkin¹⁵, Paul JR Barton^{15,16}, Zoltan Arany⁴, Michal Pravenec¹², Enrico Petretto^{1,17}, Daniel Sanchis², and Stuart A. Cook^{1,16}

¹Medical Research Council Clinical Sciences Centre, Faculty of Medicine, Imperial College London, Hammersmith Hospital, Du Cane Road, London W12 ONN, UK

²Cell Signaling & Apoptosis Group, University Lleida, Biomedical Research Institute of Lleida (IRBLLEIDA), Av Rovira Roure, 80, 25198 Lleida, Spain

³Platform of Applied Research on Laboratory Animal Barcelona Science Park, Baldiri Reixac, 4, 08028 Barcelona, Spain

⁴Cardiovascular Institute, Beth Israel Deaconess Medical Institute, CLS906, 3 Blackfan Circle, Boston MA 02215, USA

⁵Department of Radiological, Oncological and Anatomic-Pathological Sciences, Sapienza, University of Rome, Italy

⁶School of Clinical and Experimental Medicine, College of Medical and Dental Sciences, University of Birmingham, Edgbaston, Birmingham, B15 2TT

⁷Unitat de Patologia Mitocondrial i Neuromuscular, Institut de Recerca Hospital Universitari Vall d'Hebron, Universitat Autònoma de Barcelona, Barcelona, Spain

⁸Max-Delbrück Center for Molecular Medicine, Robert-Rössle-Strasse 10, 13125 Berlin, Germany

⁹CC4, Campus Charité Mitte, Charité - Universitätsmedizin Berlin, Charitéplatz 1, 10117 Berlin, Germany

¹⁰Department of Physiology, Medical College of Wisconsin, Milwaukee WI 53226, U.S.A.

¹¹Institute of Laboratory Animals, Graduate School of Medicine, Kyoto University, Yoshidakonoe-cho, Sakyo-ku, Kyoto 606-8501, Japan

¹²Institute of Physiology, Academy of Sciences of the Czech Republic, Vídenska 1083, 142 20 Prague 4, Czech Republic

¹³Grup de Patologia Cardiovascular, Institut de Recerca Hospital Universitari Vall d'Hebron, Universitat Autònoma de Barcelona, Barcelona, Spain

Correspondence and requests: stuart.cook@imperial.ac.uk or daniel.sanchis@cmb.udl.cat.

Author contributions C.M-R, J.Y., X-M.S., A.S., J.Z., A.B., R.B., D.H., H.L., G.C.R., R.M. and E.G-A. performed the lab-based experiments. R.A, P.M., M.M., V.Z., F.P, M.C., M.R-M. and F.K. performed the physiology experiments. N.H., H.J., L.E.F., P.J.R.B. and T.S., provided gene expression and physiology data. J.W, L.B. and E.P. performed genetic mapping and network studies. X.C., J.X.C., Z.A., M.P. and D.C-D. supervised data analysis and contributed to the experimental design. S.A.C and D.S. planned the experiments. S.A.C. wrote the manuscript with input and discussion from all co-authors.

¹⁴Cell Signaling & Apoptosis Group at CIBERNED and Vall d'Hebron Institut of Research (VHIR) and Dept Biochemistry-molecular Biology and Institut de Neurociències at Universitat Autònoma de Barcelona, Barcelona, Spain

¹⁵Heart Science Centre, National Heart and Lung Institute, Imperial College London, Harefield Hospital, Harefield, Middlesex, UB9 6JH, UK

¹⁶Cardiovascular Biomedical Research Unit, Royal Brompton and Harefield NHS Trust, Sydney Street, London, SW3 6NP

¹⁷Department of Epidemiology and Biostatistics, Faculty of Medicine, Imperial College London, Praed Street, London W2 1PG, UK

Abstract

Left ventricular mass (LVM) is a highly heritable trait¹ and an independent risk factor for all-cause mortality². To date, genome-wide association studies (GWASs) have not identified the genetic factors underlying LVM variation³ and the regulatory mechanisms for blood pressure (BP)-independent cardiac hypertrophy remain poorly understood^{4,5}. Unbiased systems-genetics approaches in the rat^{6,7} now provide a powerful complementary tool to GWAS and we applied integrative genomics to dissect a highly replicated, BP-independent LVM locus on rat chromosome 3p. We identified endonuclease G (*Endog*), previously implicated in apoptosis⁸ but not hypertrophy, as the gene at the locus and demonstrated loss-of-function mutation in *Endog* associated with increased LVM and impaired cardiac function. Inhibition of *Endog* in cultured cardiomyocytes resulted in an increase in cell size and hypertrophic biomarkers in the absence of pro-hypertrophic stimulation. Genome-wide network analysis unexpectedly inferred *ENDOG* in fundamental mitochondrial processes unrelated to apoptosis. We showed direct regulation of *ENDOG* by *ERRα* and *PGC1α*, master regulators of mitochondrial and cardiac function^{9,10,11}, interaction of *ENDOG* with the mitochondrial genome and *ENDOG*-mediated regulation of mitochondrial mass. At baseline, *Endog* deleted mouse heart had depleted mitochondria, mitochondrial dysfunction and elevated reactive oxygen species (ROS), which was associated with enlarged and steatotic cardiomyocytes. Our studies establish further the link between mitochondrial dysfunction, ROS and heart disease and demonstrate a new role for *Endog* in maladaptive cardiac hypertrophy.

Elevated left ventricular mass (LVM) is a clinically important trait that independently predicts the risk of heart failure, sudden death and all-cause mortality². Although LVM is a heritable complex trait¹, large genome wide association studies (GWASs) have not identified new LVM genes³. Blood pressure (BP)-dependent regulation of LVM, which is perhaps surprisingly limited⁷, has been studied extensively in model systems and acts through well-characterised and overlapping signalling modules¹². In contrast, the pathways underlying BP-independent cardiac hypertrophy, commonly seen in obesity and type 2 diabetes and related to mitochondrial dysfunction and lipotoxicity^{4,5}, remain largely unknown. Here, we took advantage of the recent step-changes in integrative systems-genetics approaches in the rat^{6,7} to dissect a BP-independent cardiac mass quantitative trait locus (QTL) and identified the causative gene and underlying mechanism.

The rat is unique for the study of cardiac mass with over 75 QTLs identified for this trait (rat genome database; <http://rgd.mcw.edu/>). Rat chromosome 3p (0-25Mbp) contains a highly replicated and BP-independent QTL for cardiac mass, which was mapped in crosses of the Spontaneously Hypertensive Rat (SHR) or SHR Stoke Prone (SHRSP) to Wistar Kyoto (WKY) or Salt Sensitive (SS)^{13,14}. To dissect genetically this locus, we generated an F₂ intercross from SHR and Brown Norway (BN) strains and replicated further the LVM QTL (LOD=4.2) (Fig. 1a). We confirmed the BP-independent QTL effect in a congenic strain

(SHR.BN-(3L)) that had lower LVM and smaller cardiomyocytes than the SHR (Fig. 1b,c) and refined the QTL region (6.4Mbp-11.2Mpb) using a second congenic strain (SHR.BN-(3S)) (Supplementary Fig. 1). In the F₂ cross, in the SHR.BN-(3L) strain and in previous experimental crosses^{13,14}, the SHR allele at the locus was associated with increased cardiac mass and this effect was BP-independent (Fig. 1a and d). Functional assessment *in vivo* revealed that the SHR.BN-(3L) strain had better cardiac performance at baseline and following stimulation, as compared to the SHR (Supplementary Fig. 1). These data demonstrate that an SHR allele at the cardiac mass QTL on rat chromosome 3p increases LVM and adversely affects cardiac function.

We used the new genotypes generated in our F₂ cross and those from previous experiments^{13,14} to refine the QTL region, and identified five distinct loci (spanning 750kbp in total) that co-segregated with the haplotypes associated with LVM variation (Fig. 1e). *Endonuclease G (Endog)*, which we had previously shown to be *cis*-regulated in the heart ($P=3\times 10^{-6}$)⁷, was the only gene at the loci to be differentially regulated with consistent direction of effect in the SHR and SHRSP heart as compared to the WKY heart (Supplementary Table 1). *Endog* is a nuclear-encoded, mitochondrial-localised nuclease with a proposed but disputed function in apoptosis^{8,15,16,17} and no known effect on cardiac mass or function. We observed reduced expression of *Endog* transcript and lack of Endog protein in all strains with elevated cardiac mass (Fig. 1f and g). Sequencing of *Endog* revealed promoter and coding sequence variation and we identified an SHR-specific, frameshift-causing insertion in *Endog* exon one that was associated with increased heart weight and LVM (Supplementary Fig. 2). There was marked reduction in cardiac nuclease activity, which was *Endog*-dependent¹⁸, in SHR heart as compared to BN heart (Fig. 1h and i). In recombinant inbred strains derived from the SHR and BN^{6,7} we confirmed the direct relationship between the SHR insertion and the lack of nuclease activity (Fig. 1j) and mapped *Endog*-dependent nuclease activity to a single locus that encodes *Endog* (Fig. 1k). These data identify *Endog* as the candidate gene at the QTL and infer *Endog* loss-of-function as the mechanism for increased cardiac mass and impaired heart function.

We performed immunoblotting across rat and mouse tissues and determined that *Endog* was most highly expressed in the heart, localised to cardiomyocytes (Fig. 2) and co-localised with mitochondria (Supplementary Fig. 3). Using short hairpin RNA (shRNA) knockdown of *Endog* (*shEndog*)¹⁹ we tested the effect of *Endog* loss-of-function in cardiomyocytes and observed an increase in hypertrophic biomarkers and cell size in the absence of pro-hypertrophic stimulation (Fig. 2). Conventional BP-dependent hypertrophic signalling pathways¹² were not activated in *shEndog* treated cells but we established activation of AMPK (Supplementary Fig. 4), which can induce cardiac hypertrophy²⁰. We also observed increased reactive oxygen species (ROS), an additional pro-hypertrophic stimulus²¹ that acts through multiple downstream effectors (Supplementary Fig. 4). These data show that *Endog* loss-of-function directly induces cardiac myocyte hypertrophy *in vitro* that is associated with the activation of two pro-hypertrophic pathways both of which have previously been linked with mitochondrial dysfunction^{20,21,22}.

We then examined the effects of *Endog* loss-of-function *in vivo* in the *Endog* deleted mouse (*Endog*^{-/-})¹⁷ that exhibits no detectable variation in apoptotic phenotypes, an observation that was confirmed in an independent *Endog* deleted strain¹⁶. As compared to controls, *Endog*^{-/-} mice had larger cardiomyocytes at baseline (Fig. 2) in the absence of stimulation, in keeping with our observations in the SHR.BN-(3L) rat (Fig. 1) and *in vitro* (Fig. 2). Following angiotensin II stimulation of hypertrophy, which is largely ROS-dependent²¹, we observed an increase in cardiomyocyte size, hypertrophic biomarkers and LVM in *Endog*^{-/-} mice (Fig. 2 and Supplementary Fig 5). *Endog*^{-/-} mice had BPs equivalent to control mice at baseline ($P=0.49$) and following angiotensin II stimulation ($P=0.51$). Our combined *in vitro*

and *in vivo* data confirm a role for *Endog* in cardiomyocyte hypertrophy and identify ROS as a conserved pro-hypertrophic stimulus in both systems.

Endog was proposed⁸ but subsequently disputed^{16,17} as important for apoptotic cell death and it was unclear how *Endog* loss-of-function was associated with cardiac hypertrophy and dysfunction. To infer *ENDOG* function in the human heart, we carried out genome-wide coexpression network analysis²³ in a large human cardiac expression dataset (n=210) (Supplementary Methods). *ENDOG* was identified in a network that was highly enriched for mitochondrial genes ($P=1.8\times 10^{-58}$) and oxidative metabolism processes ($P=4.7\times 10^{-38}$) (Fig. 3) (Supplementary Tables 2 and 3). Taken together, the high levels of *Endog* expression in metabolically active organs (Fig. 2) and in brown fat (Supplementary Fig. 6), the unique co-expression of *ENDOG* with oxidative metabolism genes and the link with AMPK signalling and ROS production pointed to an unappreciated effect of *Endog* in physiological mitochondrial processes.

Peroxisome proliferator activated receptor gamma coactivator 1 alpha (*Pgc1 α*) is widely recognised as a master regulator of mitochondrial function²⁴, and activates many target genes component of the *ENDOG*-associated network (Fig. 3) through interaction with estrogen-related receptor alpha (*Err α*)⁹. Therefore, we tested whether *Pgc1 α* also regulated *Endog* and observed robust *Pgc1 α* -induced *Endog* transcript and *Endog* protein expression in cardiomyocytes *in vitro* (Fig. 3). We confirmed the effects of *Pgc1 α* variation on *Endog* protein expression *in vivo* using mice over-expressing *Pgc1 α* under the control of muscle creatine kinase (MCK-*Pgc1 α*) and in cardiac-specific *Pgc1 α* deleted mice (*Pgc1 α* ^{$\Delta C/\Delta C$}) (Fig. 3, Supplementary Methods). Luciferase studies revealed strong activation of the *Endog* promoter by *Pgc1 α* and *Err α* together (Fig. 3e) and we confirmed direct binding of *ESRR α* to the *ENDOG* promoter by chromatin immuno-precipitation and PCR (ChIP-PCR) in a region containing an *ERR α* response element ($P<0.001$) (Fig. 3f). These data show that *Endog* is a direct target of *ESRR α* and *Pgc1 α* , master regulators of mitochondrial and heart function, further inferring a role for *Endog* in mitochondrial and cardiac biology.

It was apparent that the effects of *Endog* loss-of-function on cardiac hypertrophy might be mediated through perturbation of mitochondrial physiology, which we examined. Electron microscopy revealed no gross morphological changes of mitochondria but we observed lipid-like droplets associated with mitochondria from *Endog*^{-/-} mice that were more numerous and larger than those seen in control mice. Molecular studies revealed marked elevation of triglyceride levels in the *Endog*^{-/-} mouse heart that was manifest as cardiomyocyte steatosis (Fig. 4 and Supplementary Fig. 7) but not associated with variation in expression levels of fatty acid metabolism or mitochondrial biogenesis genes (Supplementary Fig. 8 and 9). As compared to wildtype littermates, *Endog*^{-/-} mice had impaired mitochondrial respiration and increased ROS production (Fig. 4).

To assess for mitochondrial depletion we examined mitochondrial DNA (mtDNA)/genomic DNA and mitochondrial protein/tissue weight ratios, which were both diminished in the *Endog*^{-/-} mouse heart (Fig. 4) in the absence of mtDNA structural variation (Supplementary Fig. 10). This was an intriguing finding given the previously proposed roles for *Endog* in mtDNA synthesis, processing of poly-cistronic mtRNA and mitochondrial biogenesis^{25,26} that were subsequently discarded based primarily on experiments in *Endog* deleted mice^{16,17}. We re-examined a role of *ENDOG* in mitochondrial biogenesis and demonstrated an increase in mitochondrial mass with chronic *ENDOG* expression in HEK cells ($P<0.01$) and acute *Endog* over-expression in a cardiomyocyte-derived cell line ($P<0.001$) (Fig. 4k-k in the absence of an effect on apoptotic or necrotic cell death (Supplementary Fig. 11). A role for *ENDOG* in mtDNA biology^{25,26} was supported further by ChIP-PCR experiments that showed direct binding of *ENDOG* throughout the mtDNA molecule (Fig.

4n) as previously demonstrated for mitochondrial transcription factor A (TFAM)²⁷, which is a critical determinant of mtDNA synthesis and repair that when deleted causes eccentric cardiac hypertrophy and heart failure²⁸.

Mitochondria are essential for oxidative metabolism and mitochondrial dysfunction/depletion in the heart causes maladaptive cardiac hypertrophy and cardiac dysfunction associated with increased ROS and lipotoxicity^{4,5,28,29}. Here we identified *Endog* loss-of-function as a primary determinant of maladaptive cardiac hypertrophy that was associated with mitochondrial dysfunction/depletion and marked cardiomyocyte steatosis. Although the mechanism underlying cardiac hypertrophy due to impaired mitochondrial function is not limited to a single pathway we demonstrated a conserved increase in ROS, an established hypertrophic stimulus^{21,22}, in *Endog* loss-of-function models. Our studies resolve some of the uncertainty as to the non-apoptotic function of *Endog*^{15,16,17} and reveal its importance in mitochondrial biology, which has intriguing parallels with the dual roles of apoptosis-inducing-factor³⁰. We propose that *ENDOG*, which we show binds to mtDNA, modulates mtDNA synthesis, maintenance and/or transcription, in keeping with previous hypotheses^{25,26}. Therapeutic targeting the *Pgc1 α /Err α* axis has been proposed to improve mitochondrial function in cardiac failure¹¹ and our studies suggest that regulation of *Endog* is an important component of this process. We conclude that *Endog* is a novel determinant of maladaptive cardiac hypertrophy with previously unappreciated mitochondrial functions.

Methods Summary

Linkage mapping was carried out using microsatellite genotypes in the BNxSHR F₂ population. *Ex vivo* heart weight analysis was performed in the congenic strains, which were characterised using *in vivo* BP telemetry. Comparative haplotype analysis was performed using SNP data (Rat Genome Database; <http://rgd.mcw.edu/>) for all strains used in the QTL mapping studies. Microarray-based expression analysis was conducted as previously described^{6,7}. Cell size and hypertrophy biomarker expression were measured in cardiomyocytes following lentivirus-mediated *Endog* knockdown. Heart weight, hypertrophic biomarker expression and cardiomyocyte cell size were measured in *Endog*^{-/-} mice at baseline and following angiotensin II-induced hypertrophy. Triglyceride abundance, mitochondrial mass and respiratory activity were measured in *Endog*^{-/-} mice as described in the Supplementary material. Weighted gene co-expression network analysis (WGCNA)²³ was applied to the largest publicly available human heart transcriptome dataset. Regulation of *Endog* by *Pgc1 α* was investigated in Ad.*Pgc1 α* -infected neonatal cardiomyocytes, MCK-*Pgc1* skeletal muscle and *Pgc1* $\alpha^{AC/AC}$ heart samples. ERR α association with the *ENDOG* promoter and *ENDOG*-mtDNA interaction were determined using ChIP. Histological analysis and electron microscopy of *Endog*^{-/-} hearts was carried out to study mitochondrial structure and abundance as well as lipid deposition. MtDNA and gDNA copy number were assessed by QPCR. Mitochondrial abundance was studied in cells by flow cytometry. Full methods are provided in Supplementary Methods.

Supplementary Material

Refer to Web version on PubMed Central for supplementary material.

Acknowledgments

We acknowledge funding from the Medical Research Council (MRC) UK, the National Institute for Health Research (NIHR) UK, the Royal Brompton and Harefield Cardiovascular Biomedical Research Unit, the Imperial College Healthcare Biomedical Research Centre, the British Heart Foundation, the Fondation Leducq, the Wellcome Trust, 301/08/0166 from the Grant Agency of the Czech Republic and 1M0520 from the Ministry of Education of the Czech Republic, PTQ-08-03-07880, SAF2008-02271, SAF2008-03067 and SAF2010-19125 from

the Ministerio de Ciencia e Innovacion (MICINN, Spain), 2009-SGR-346 from the Agència de Gestió d'Ajuts Universitaris i Recerca (AGAUR, Spain), PS09/02034, PS09/01602 and PS09/01591 from Fondo de Investigaciones (FIS, Spain). The European Community's Seventh Framework Programme (FP7/2007-2013) under grant agreement no. HEALTH-F4-2010-241504 (EURATRANS). The German National Genome Research Network (NGFN-Plus) Heart Failure. We thank Dr Michael R. Lieber (University of Southern California) for providing the *Endog* deleted mice and Prof E. Wahle (Institute of Biochemistry and Biotechnology, Halle) for providing the CG4930 expression plasmid. We thank the National BioResource Project-Rat (<http://www.anim.med.kyoto-u.ac.jp/NBR/>) for providing rat strains.

References

1. Post WS, Larson MG, Myers RH, Galderisi M, Levy D. Heritability of left ventricular mass: the Framingham Heart Study. *Hypertension*. 1997; 30:1025–1028. [PubMed: 9369250]
2. Lorell BH, Carabello BA. Left ventricular hypertrophy: pathogenesis, detection, and prognosis. *Circulation*. 2000; 102:470–479. [PubMed: 10908222]
3. Vasan RS, et al. Genetic variants associated with cardiac structure and function: a meta-analysis and replication of genome-wide association data. *JAMA*. 2009; 302:168–178. [PubMed: 19584346]
4. McGavock JM, Victor RG, Unger RH, Szczepaniak LS. Adiposity of the heart, revisited. *Ann Intern Med*. 2006; 144:517–524. [PubMed: 16585666]
5. Wong C, Marwick TH. Obesity cardiomyopathy: pathogenesis and pathophysiology. *Nat Clin Pract Cardiovasc Med*. 2007; 4:436–443. [PubMed: 17653116]
6. Heinig M, et al. A trans-acting locus regulates an anti-viral expression network and type 1 diabetes risk. *Nature*. 2010; 467:460–464. [PubMed: 20827270]
7. Petretto E, et al. Integrated genomic approaches implicate osteoglycin (*Ogn*) in the regulation of left ventricular mass. *Nat Genet*. 2008; 40:546–552. [PubMed: 18443592]
8. Li LY, Luo X, Wang X. Endonuclease G is an apoptotic DNase when released from mitochondria. *Nature*. 2001; 412:95–99. [PubMed: 11452314]
9. Dufour CR, et al. Genome-wide orchestration of cardiac functions by the orphan nuclear receptors ERRalpha and gamma. *Cell Metab*. 2007; 5:345–356. [PubMed: 17488637]
10. Wu Z, et al. Mechanisms controlling mitochondrial biogenesis and respiration through the thermogenic coactivator PGC-1. *Cell*. 1999; 98:115–124. [PubMed: 10412986]
11. Finck BN, Kelly DP. PGC-1 coactivators: inducible regulators of energy metabolism in health and disease. *J Clin Invest*. 2006; 116:615–622. [PubMed: 16511594]
12. Hill JA, Olson EN. Cardiac plasticity. *N Engl J Med*. 2008; 358:1370–1380. [PubMed: 18367740]
13. Inomata H, et al. Identification of quantitative trait loci for cardiac hypertrophy in two different strains of the spontaneously hypertensive rat. *Hypertens Res*. 2005; 28:273–281. [PubMed: 16097372]
14. Siegel AK, et al. Genetic loci contribute to the progression of vascular and cardiac hypertrophy in salt-sensitive spontaneous hypertension. *Arterioscler Thromb Vasc Biol*. 2003; 23:1211–1217. [PubMed: 12775577]
15. Buttner S, et al. Endonuclease G regulates budding yeast life and death. *Mol Cell*. 2007; 25:233–246. [PubMed: 17244531]
16. David KK, Sasaki M, Yu SW, Dawson TM, Dawson VL. EndoG is dispensable in embryogenesis and apoptosis. *Cell Death Differ*. 2006; 13:1147–1155. [PubMed: 16239930]
17. Irvine RA, et al. Generation and characterization of endonuclease G null mice. *Mol Cell Biol*. 2005; 25:294–302. [PubMed: 15601850]
18. Temme C, et al. The *Drosophila melanogaster* Gene *cg4930* Encodes a High Affinity Inhibitor for Endonuclease G. *J Biol Chem*. 2009; 284:8337–8348. [PubMed: 19129189]
19. Bahi N, et al. Switch from caspase-dependent to caspase-independent death during heart development: essential role of endonuclease G in ischemia-induced DNA processing of differentiated cardiomyocytes. *J Biol Chem*. 2006; 281:22943–22952. [PubMed: 16754658]
20. Arad M, et al. Constitutively active AMP kinase mutations cause glycogen storage disease mimicking hypertrophic cardiomyopathy. *J Clin Invest*. 2002; 109:357–362. [PubMed: 11827995]

21. Dai DF, et al. Mitochondrial oxidative stress mediates angiotensin II-induced cardiac hypertrophy and Galphaq overexpression-induced heart failure. *Circ Res.* 2011; 108:837–846. [PubMed: 21311045]
22. Seddon M, Looi YH, Shah AM. Oxidative stress and redox signalling in cardiac hypertrophy and heart failure. *Heart.* 2007; 93:903–907. [PubMed: 16670100]
23. Zhang B, Horvath S. A general framework for weighted gene co-expression network analysis. *Stat Appl Genet Mol Biol.* 2005; 4 Article17.
24. Spiegelman BM. Transcriptional control of mitochondrial energy metabolism through the PGC1 coactivators. *Novartis Found Symp.* 2007; 287:60–63. discussion 63-69. [PubMed: 18074631]
25. Cote J, Ruiz-Carrillo A. Primers for mitochondrial DNA replication generated by endonuclease G. *Science.* 1993; 261:765–769. [PubMed: 7688144]
26. Tiranti V, et al. Chromosomal localization of mitochondrial transcription factor A (TCF6), single-stranded DNA-binding protein (SSBP), and endonuclease G (ENDOG), three human housekeeping genes involved in mitochondrial biogenesis. *Genomics.* 1995; 25:559–564. [PubMed: 7789991]
27. Rothfuss O, et al. Parkin protects mitochondrial genome integrity and supports mitochondrial DNA repair. *Hum Mol Genet.* 2009; 18:3832–3850. [PubMed: 19617636]
28. Wang J, et al. Dilated cardiomyopathy and atrioventricular conduction blocks induced by heart-specific inactivation of mitochondrial DNA gene expression. *Nat Genet.* 1999; 21:133–137. [PubMed: 9916807]
29. Lewis W, et al. Decreased mtDNA, oxidative stress, cardiomyopathy, and death from transgenic cardiac targeted human mutant polymerase gamma. *Lab Invest.* 2007; 87:326–335. [PubMed: 17310215]
30. Vahsen N, et al. AIF deficiency compromises oxidative phosphorylation. *EMBO J.* 2004; 23:4679–4689. [PubMed: 15526035]

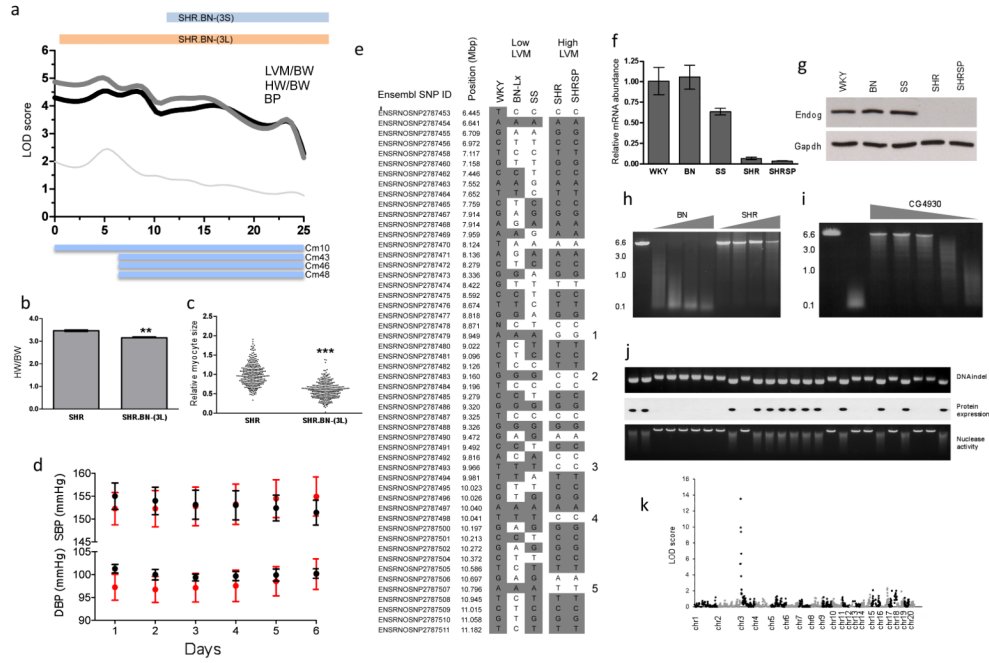


Figure 1. Positional cloning of *Endog* as the gene underlying the rat chromosome 3p cardiac mass quantitative trait locus (QTL)

a, Mapping of heart weight (HW) and left ventricular mass (LVM) corrected for body weight (BW) to chromosome 3p in the Brown Norway (BN) x Spontaneously Hypertensive (SHR) F₂ population. The telomeric limits of the congenic strains (SHR.BN-(3L) and SHR.BN-(3S)) and the previously mapped cardiac mass (CM) QTLs^{13,14} are shown; x-axis, physical position in Mbp. **b**, HW indexed to BW in the SHR (n=4) and the SHR.BN-(3L) congenic strains (n=5). **c**, Relative cardiomyocyte cross-sectional area in SHR and SHR.BN-(3L) congenic strains. **d**, *In vivo* telemetric systolic- and diastolic-blood pressure (SBP and DBP) measurements in the SHR (red circles) and SHR.BN-(3L) (black circles) (n=8 per genotype). **e**, Haplotype analysis of the refined QTL region. SNPs are depicted with reference to WKY/NCrl alleles (grey, identical; white, dissimilar) with numbers (1-5) denoting the polymorphic regions between strains with either high or low HW. QPCR of *Endog* mRNA expression (**f**) and immunoblot of *Endog* protein expression (**g**) in strains with low or high CM at the chromosome 3p locus. **h**, Nuclease activity in BN and SHR heart extracts over a range of cardiac protein extract amounts (grey wedge) (Supplementary Methods). **i**, Reversal of nuclease activity in cardiac lysates by a drosophila-derived inhibitor of *Endog*¹⁸ (range 1500nM-1.5nM, grey wedge). **j**, Association of the *Endog* indel with loss of *Endog* protein expression and diminished nuclease activity in the recombinant inbred (RI) strains. Upper, middle and lower panels display the DNA indel, protein expression and nuclease activity, respectively. **k**, Linkage mapping of nuclease activity in RI strains using a quantitative fluorescence-based assay (Supplementary Methods). All data are represented as mean+s.e.m. *, *P*<0.05, **, *P*<0.01, ***, *P*<0.001.

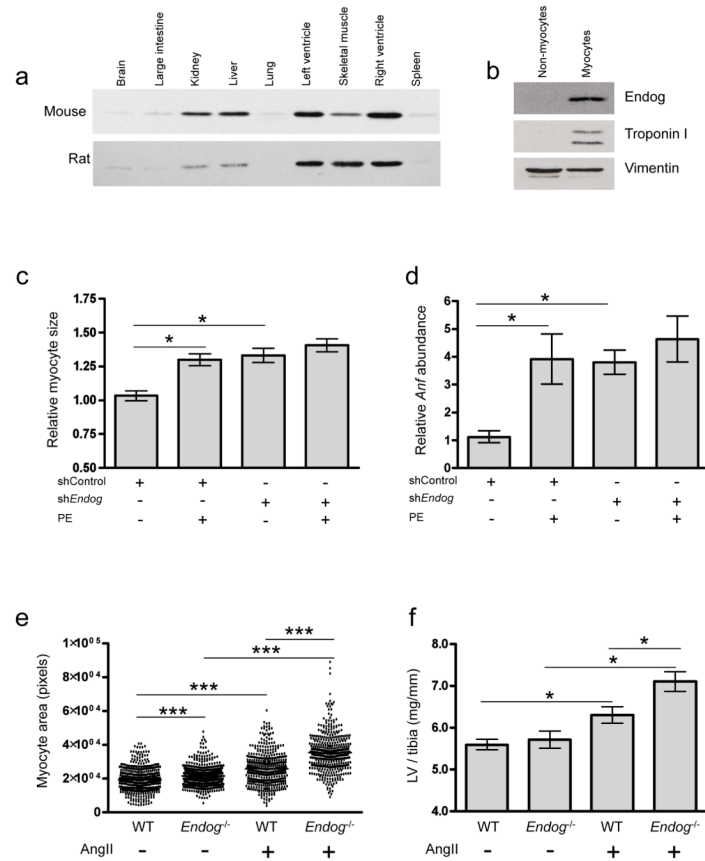


Figure 2. *Endog* regulates cardiac hypertrophy

a, Immunoblot of Endog expression in mouse and rat tissues (Endog: ~30 kDa). **b**, Immunoblot of Endog expression in myocyte and non-myocyte populations isolated from neonatal rat heart. **c**, Cardiomyocyte size (n = 100 cells, n=3 independent experiments) treated with shRNA against *Endog* (sh*Endog*) or control shRNA (shControl) in the presence or absence of the hypertrophic stimulant phenylephrine (PE, 100 μ M, 24 h). **d**, Expression of the hypertrophic biomarker *Anf* in sh*Endog* and shControl treated cells. **e**, Cardiomyocyte size (Supplementary Fig. 5) in *Endog*^{-/-} and wildtype (WT) mice at baseline and following angiotensin II-induced cardiac hypertrophy. **f**, LVM/tibial length in *Endog*^{-/-} and WT mice at baseline and following AngII stimulation. Data are represented as mean+s.e.m. *, $P < 0.05$, **, $P < 0.01$, ***, $P < 0.001$.

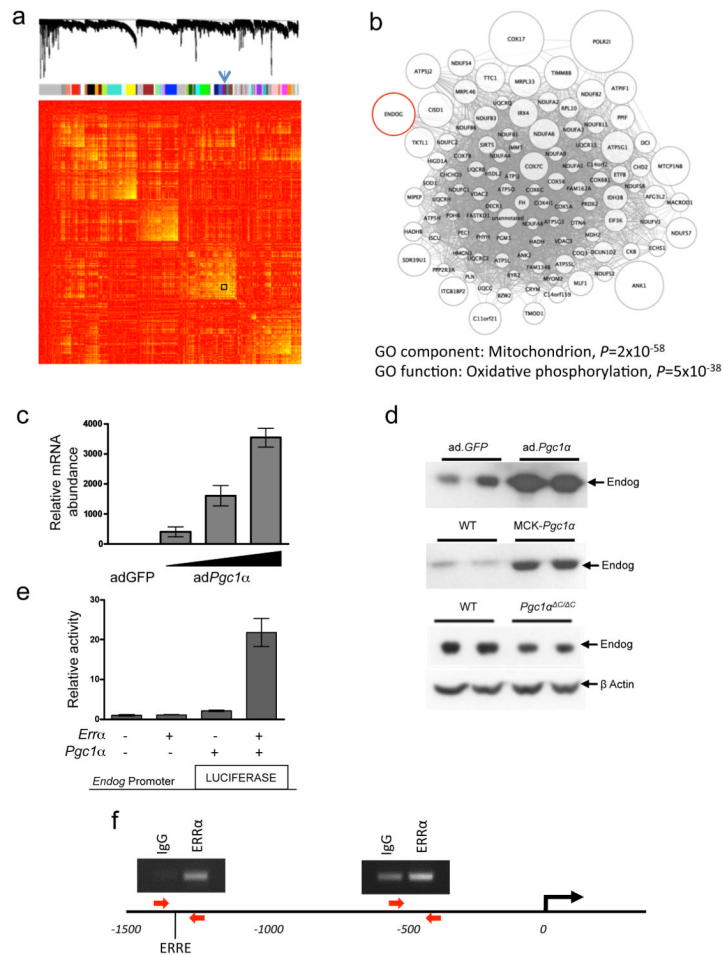


Figure 3. *ENDOG* is co-expressed with a mitochondrial-specific gene network and regulated by *Pgc1 α* and *ERR α*

a. Genes (8,490 from 210 datasets) are clustered and plotted based on the dissimilarity metric between their expression profiles (Supplementary Methods). From top to bottom: low-hanging branches in the dendrogram represent groups of genes (modules) that have a high similarity metric. Modules are shown beneath the dendrogram and are colour coded. The arrow indicates the module (also boxed) containing *ENDOG*. In the heat-map of the correlations between expression profiles, high and low similarities are coloured yellow and red, respectively. **b.** Weighted gene co-expression network analysis (WGCNA²³) for the module containing *ENDOG*, providing functional annotation by cellular localization by Gene Ontology classification (Supplementary Tables 2 and 3). Nodes represent genes and edges represent significant co-expression between genes. The node size is proportional to the relative degree of interconnectivity of each gene within the module. **c.** QPCR analysis of *Endog* expression in cultured cardiomyocytes following infection with adenovirus (ad) expressing *GFP* (ad.*GFP*) or *Pgc1 α* (ad.*Pgc1 α*). **d.** Immunoblot of *Endog* expression in ad.*Pgc1 α* -infected cardiomyocytes (top panel), skeletal muscle of wild-type (WT) mice and transgenic mice expressing *Pgc1 α* under the control of muscle creatine kinase (MCK-*Pgc1 α*) (middle panel), and in hearts of WT and cardiac-specific *Pgc1 α* deleted mice (*Pgc1 α* ^{$\Delta C/\Delta C$}) (bottom panel). **e.** *Endog* promoter activity in HEK293 cells infected with ad.*Pgc1 α* and and/or ad.*Err α* . **f.** *ERR α* chromatin immunoprecipitation (ChIP) and PCR of two regions of the *ENDOG* promoter. Red arrows denote primers and ERRE specifies the

location of a consensus ERR response element (1304 bases upstream). The experiment was repeated three times with similar results and PCR products quantified by QPCR.

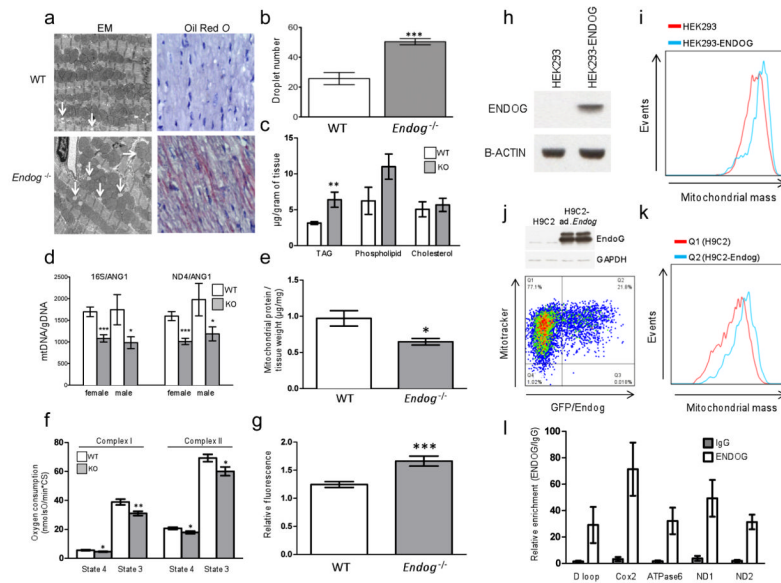


Figure 4. *Endog* regulates mitochondrial function and cardiac lipid metabolism

a, Transmission electron micrographs and oil red *O* stained micrographs (high resolution, Supplementary Fig. 7) of left ventricular sections from WT and *Endog*^{-/-} mice. **b**, Quantification of the number of mitochondrial-associated droplets in WT and *Endog*^{-/-} mice. **c**, Quantification of cardiac triglyceride (TAG), phospholipid and cholesterol content in WT and *Endog*^{-/-} mice (n=5). **d**, Ratio of mitochondrial DNA (mtDNA) to genomic DNA (gDNA) in hearts of WT and *Endog*^{-/-} mice. **e**, Quantification of mitochondrial protein content in WT and *Endog*^{-/-} mice (n=5). **f**, State 3 and state 4 oxygen consumption in the presence of complex I or complex II substrates in isolated cardiac mitochondria from WT (n=6) and *Endog*^{-/-} (n=5) mice. **g**, Relative fluorescence-based measurement of ROS production by mitochondria isolated from WT (n=6) and *Endog*^{-/-} (n=5) mice. **h-k**, Representative flow cytometry analysis of mitochondrial mass in HEK293 and H9C2 cells over-expressing ENDOG or Endog, respectively (n=4). **h**, Stable expression of ENDOG in HEK293 cells (HEK293-ENDOG). **i**, Flow cytometry analysis of HEK293 and HEK293-ENDOG cells stained with mitotracker. **j**, Adenovirus (ad)-mediated expression of GFP and Endog in myocytes and flow cytometry analysis of ad.*Endog* infected cells (Q2) and uninfected control cells (Q1). **k**, Number of events plotted against mitochondrial mass in ad.*Endog* infected (Q2) and control (Q1) H9C2 cells. **l**, QPCR of mtDNA-protein complexes following ChIP of mitochondrial chromatin using anti-ENDOG antibody or IgG. All data are represented as mean+s.e.m. *, *P*<0.05, **, *P*<0.01, ***, *P*<0.001.